

Experimental investigation and thermodynamic calculation of the Ga–Sb–Zn phase diagram

Irma Dervišević · Andreja Todorović ·
Nada Talić · Jelena Djokić

Received: 23 June 2009 / Accepted: 9 November 2009 / Published online: 6 February 2010
© Springer Science+Business Media, LLC 2010

Abstract Phase equilibrium of ternary Ga–Sb–Zn system was investigated by applying CALPHAD method and using literature thermodynamic data for constitutive binary systems. The liquidus surface and isothermal section at 673 K were calculated. Calculated results were verified experimentally on the alloys samples with the compositions corresponding to the characteristic vertical sections: SbZn (1:1)–Ga; GaZn(1:1)–Sb; and GaSb(1:1)–Zn. Phase transitions temperatures were determined by differential thermal analysis and differential scanning calorimetry. Microstructure and phase composition investigation were investigated by using scanning electronic microscopy with energy dispersive spectrometry. The experimental and analytical results showed good agreement, concerning the temperatures of phase transitions and phase compositions of alloys concerned.

Introduction

There is a significant importance of the ternary Ga–Sb–Zn system, as one of the GaSb-based systems, considering the development of optoelectronic devices [1]. In order to develop a simple and reproducible method to fabricate p–n-type of GaSb for optoelectric devices, zinc diffusion

into *n*-doped GaSb substrates was studied by Bett et al. [1]. They investigated Zn diffusion from the vapor phase and from the liquid phase, and process parameters, which provide good control over Zn surface concentration were obtained. Bracht et al. [2] investigated self-diffusion of Ga and Sb in undoped GaSb and revealed that Ga diffuses faster than Sb by several orders of magnitude. The diffusion behavior of Zn in *n*-type GaSb was investigated by Sundarem [3] and Nicols [4]. Conibeer [5] investigated zinc diffusion in tellurium doped GaSb, with the aim of constructing of booster cell. The study of Suliman [6] is referring to the fabrication and simulation of GaSb photovoltaic cells, while

Table 1 Considered phases and their crystal structures [17]

Phase-common names	Thermodynamic database name	Pearson's symbol
L	LIQUID	Not applicable
(Ga)	ORT	oC8
(Sb)	RHOMBOHEDRAL_A7	hR2
GaSb	FCC_B3	cF8
(Zn)	HCP_ZN	hP2
β	BETA_SBZN	oP16
γ	GAMMA_SBZN	...
ε	EPSILON_SBZN	(a)
δ	DELTA_SBZN	(a)
ζ	ZETA_SBZN	oP ^a
η	ETA_SBZN	oP30

(a)—marks that in listed ε and δ phases Pearson's symbols were not completely determined in literature and it can be either hR22 or oP28 (Bravais' lattice is either rhombohedral (hR) with 22 atoms in elemental cell or orthorhombic (oP) with 28 atoms in elemental cell)

^a Unknown number of atoms in elemental cell

I. Dervišević (✉) · A. Todorović · J. Djokić
Faculty of Technical Sciences, University of Pristina,
38220 Kosovska Mitrovica, Serbia
e-mail: ir-mader-visevic@hotmail.com

N. Talić
Institute of Chemistry, Technology and Metallurgy,
Njegoševa 12, 11000 Belgrade, Serbia

Luca [7] investigated thermophotovoltaic devices. The development of ceramic semiconductor processes [8] were also concerned to the system. All these studies pointed out the importance of definition of ternary Ga–Sb–Zn system.

Mirgalovskaya and Komova [9] have determined liquid projection of the ternary Ga–Sb–Zn system, with seven small primary crystallization fields ((Zn), (Ga), Zn_3Sb_2ht1 , Zn_3Sb_2ht2 , $Zn_{6,3}Sb_{4,7}ht$, ZnSb, and (Sb)) and one large crystallization field (GaSb). Five invariant reactions were determined, two of them were E-type, and three of them were U-type reactions.

The investigations of binary and ternary phase diagrams were recently presented by many authors [10–13].

In this article, the temperatures of phase transition for three vertical sections of ternary Ga–Sb–Zn system, determined by differential scanning calorimetry (DSC) and differential thermal analysis (DTA) methods, are presented. The microstructures and the compositions of equilibrium phases were obtained by scanning electron microscopy (SEM)–EDS. The experimentally determined values of the phase transition temperatures were compared to the calculated ones based on optimized thermodynamic

Table 2 Optimized thermodynamic parameters for constitutive binaries used in this study

Optimized thermodynamic parameters	References
LIQUID—constituents: GA,SB,ZN	
$L(LIQUID,GA,ZN;0) = +3662.8 + 27.28629 * T - 4.2 * T * LN(T)$	[15]
$L(LIQUID,GA,ZN;1) = -464.2$	[15]
$L(LIQUID,GA,SB;0) = -13953.8 + 71.0787 * T - 9.6232 * T * LN(T)$	[14]
$L(LIQUID,GA,SB;1) = +1722.9 - 1.92588 * T$	[14]
$L(LIQUID,GA,SB;2) = 2128.3$	[14]
$L(LIQUID,SB,ZN;0) = -11740.942 - 0.1283 * T$	[16]
$L(LIQUID,SB,ZN;1) = -427.582 - 0.809855 * T$	[16]
$L(LIQUID,SB,ZN;2) = +34440.943 - 33.59286 * T$	[16]
ORT—2 sublattices, sites 1: 1, constituents: GA: VA	
$G(ORT,GA:VA;0) - H298(ORT,GA;0) = +GHSERGA$	[14]
RHOMBOHEDRAL_A7, constituents: SB,ZN	
$L(RHOMBOHEDRAL_A7,SB,ZN;0) = 0.0$	[16]
FCC_B3—2 sublattices, sites 0.5: 0.5, constituents: GA: SB	
$G(FCC_B3,GA:SB;0) - 0.5 H298(ORT,GA;0) - 0.5 H298(RHOMBOHEDRAL_A7,SB;0) = -21738.1 - 10.53764 * T + 2.692876 * T * LN(T) - 0.00137791 * T ** 2 + 0.5 * GHSERGA + 0.5 * GHSERSB$	[14]
HCP_ZN—2 sublattices, sites 1: 0.5, constituents: GA, ZN: VA	
$L(HCP_ZN,GA,ZN:VA;0) = 10744$	[15]
BETA_SBZN—2 sublattices, sites 0.5: 0.5, constituents: SB: ZN	
$G(BETA_SBZN,SB:ZN;0) - 0.5 H298(RHOMBOHEDRAL_A7,SB;0) - 0.5 H298(HCP_A3,ZN;0) = -11542.68 + 5 * T + 0.5 * GHSERZN + 0.5 * GHSERSB$	[15]
GAMMA_SBZN—2 sublattices, sites 0.45: 0.55, constituents: SB: ZN	
$G(GAMMA_SBZN,SB:ZN;0) - 0.45 H298(RHOMBOHEDRAL_A7,SB;0) - 0.55 H298(HCP_A3,ZN;0) = -8748.7632 + 1.3365 * T + 0.45 * GHSERSB + 0.55 * GHSERZN$	[15]
EPSILON_SBZN—2 sublattices, sites 0.425: 0.575, constituents: SB: ZN	
$G(EPSILON_SBZN,SB:ZN;0) - 0.425 H298(RHOMBOHEDRAL_A7,SB;0) - 0.575 H298(HCP_A3,ZN;0) = -7730.454 + 0.425 * GHSERSB + 0.575 * GHSERZN$	[15]
DELTA_SBZN—2 sublattices, sites 0.425: 0.575, constituents: SB: ZN	
$G(DELTA_SBZN,SB:ZN;0) - 0.425 H298(RHOMBOHEDRAL_A7,SB;0) - 0.575 H298(HCP_A3,ZN;0) = -7348 - 0.5 * T + 0.425 * GHSERSB + 0.575 * GHSERZN$	[15]
ZETA_SBZN—2 sublattices, sites 0.4: 0.6, constituents: SB: ZN	
$G(ZETA_SBZN,SB:ZN;0) - 0.4 H298(RHOMBOHEDRAL_A7,SB;0) - 0.6 H298(HCP_A3,ZN;0) = -4918.01 - 3.37557 * T + 0.4 * GHSERSB + 0.6 * GHSERZN$	[15]
ETA_SBZN—2 sublattices, sites 0.38: 0.62, constituents: SB: ZN	
$G(ETA_SBZN,SB:ZN;0) - 0.38 H298(RHOMBOHEDRAL_A7,SB;0) - 0.62 H298(HCP_A3,ZN;0) = -5042.71 - 2.743826 * T + 0.38 * GHSERSB + 0.62 * GHSERZN$	[15]

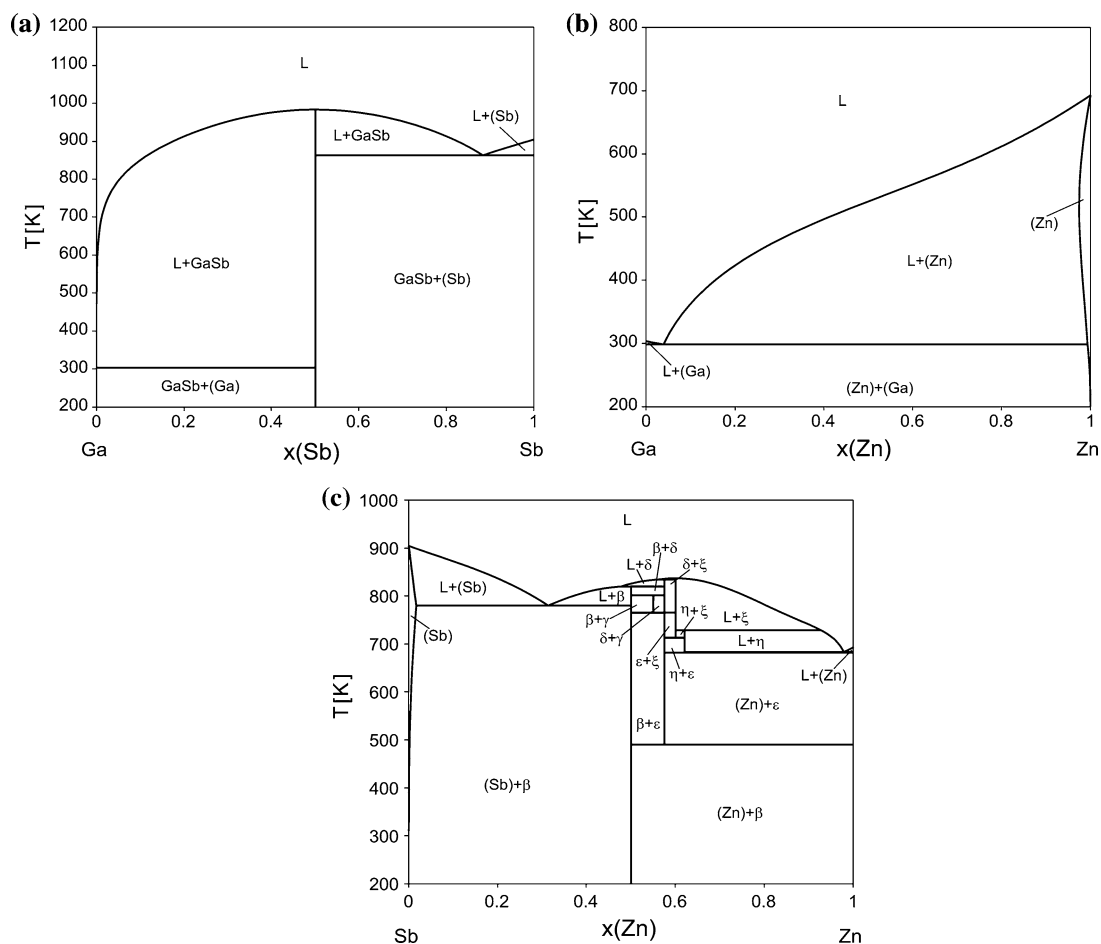


Fig. 1 Phase diagrams of the constitutive binary systems: **a** Ga–Sb, **b** Ga–Zn, **c** Sb–Zn

data for constitutive binary systems [14–16], by using software package PANDAT 8.1.

The results obtained in this work represent a step forward to the complete definition of phase diagram of ternary Ga–Sb–Zn system, which was incompletely investigated, and have a potential for wide technological application.

Experimental

The alloy samples were prepared from high-purity (99.999%) gallium, antimony, and zinc produced by Alfa Aesar (Germany). Selected samples with compositions from three vertical sections are with molar ratio of two components of 1:1. Molar ratio of the third component was in a range of 0 to 1, with portion of 0.1. The samples were prepared as following: the mixtures (~2 g) of the metals were well grained and sealed in quartz tubes under a

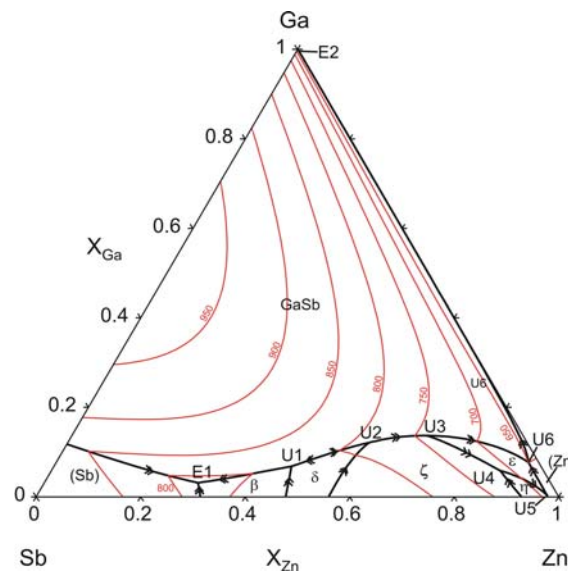


Fig. 2 Calculated liquidus surface of the ternary Ga–Sb–Zn system

vacuum and placed in a resistance furnace. The sealed tubes containing the mixed elements were gradually heated to the melting point of Sb (903.85 K). The samples were well stirred and then held at that temperature for 30 min. The quartz tubes were taken out of furnace and left for cooling in the air to the room temperature. After that, the sealed quartz tubes with the samples, which were planned for SEM–EDS analysis, were heated in electric resistance furnace until the annealing temperature of 673 K was reached. At this temperature, the samples were annealed over a period of 200 h, and immediately quenched in icy water.

The phase transformation temperatures were determined by DTA and DSC methods. The DTA measurements were carried out on Derivatograph (MOM Budapest) under following conditions: flowing argon atmosphere, sample masses about 1 g, alumina as the reference material, heating rate of 5 K/min. The DSC measurements were performed on a SDT Q600 (TA Instruments), under flowing argon atmosphere, with sample masses 50 mg, and heating rate of 5 K/min.

For microstructure investigation and for phase composition determination was used SEM (JEOL JSM 6460) with energy dispersive spectrometry (EDS) (Oxford Instruments).

Thermodynamic models

The phases from constitutive binary subsystems considered for thermodynamic binary-based prediction with their Pearson's symbols are listed in Table 1.

Phase diagram of the Ga–Sb–Zn ternary system was calculated by the CALPHAD method, using only optimized thermodynamic parameters for constitutive binary systems. The CALPHAD method for the calculation of thermodynamic equilibrium is based on modeling the Gibbs energies of all phases in the investigated system and, minimizing the total Gibbs energy of the system.

Thermodynamic models and parameters used for calculation of the Bi–Ga–Sb phase diagram are shown in Table 2.

The stable forms of the pure elements at 298.15 K and 1 bar were chosen as the reference states of the system. For the thermodynamic functions of the pure elements in their stable and metastable states were used the phase stability equations, compiled by Dinsdale [18]. Literature thermodynamic data were taken for the system Ga–Sb from Ansare et al. [14], for the system Ga–Zn from Dutkiewicz et al. [15], and for the system Sb–Zn from Liu [16]. The Gibbs energies of intermediate phases: GaSb, β , γ , ε , δ , ζ and η were modeled by sublattice model [19, 20]. The

phase diagrams for the constitutive binary systems were calculated by application of the software package PAN-DAT 8.1, and presented on Fig. 1.

Table 3 Predicted invariant reaction of ternary Ga–Sb–Zn system

T (K)	Reaction	Type
803.18	$L \rightleftharpoons \beta + \text{GaSb} + \delta$	U1
784.92	$L + \delta \rightleftharpoons \text{GaSb} + \zeta$	U2
772.49	$L \rightleftharpoons (\text{Sb}) + \beta + \text{GaSb}$	E1
739.41	$\text{GaSb} + \zeta \rightleftharpoons L + \varepsilon$	U3
712.64	$L + \zeta \rightleftharpoons \varepsilon + \eta$	U4
681.25	$L + \eta \rightleftharpoons \varepsilon + (\text{Zn})$	U5
649.49	$L + \varepsilon \rightleftharpoons (\text{Zn}) + \text{GaSb}$	U6
297.85	$L \rightleftharpoons \text{GaSb} + (\text{Zn}) + (\text{Ga})$	E2

Table 4 Phase transition temperatures obtained by using DTA and DSC methods

Sample composition	Phase transition temperatures (K)	
	Liquidus temperature	Other phase transition temperature
X_{Ga}	$X_{\text{Sb}}/X_{\text{Zn}} = 1$	
0.1	822.2	493; 754.4; 805.3
0.2	856.7	663.1; 749.4; 768.1; 805.1
0.3	867.0	642.3; 741.4
0.4	890.1	297.5; 626.9
0.5	897.5	304.2; 552.4
0.6	865.2	301.2; 482.4
0.7	862.2	292.5; 427.9
0.8	856.5	299.3,
0.9	801.6	308.5
X_{Sb}	$X_{\text{Ga}}/X_{\text{Zn}} = 1$	
0.1	749.2	312.4; 517.4
0.2	817.5	302.2; 516.8
0.3	876.1	309.8; 520.3,
0.4	893.9	489.3; 657.3; 751.2; 775.8; 781.5
0.5	912.8	794.3
0.6	894.7	777.6
0.7	876.2	766.2; 816.4
0.8	841.8	775.2; 817.6
0.9	856.9	827.4
X_{Zn}	$X_{\text{Ga}}/X_{\text{Sb}} = 1$	
0.1	964.4	641.2; 702.4
0.2	913.2	654.3; 726.2
0.3	897.4	655.1; 721.1
0.4	835.8	652.3; 731.5
0.5	807.1	656.9
0.6	774.4	659.2
0.7	731.4	644.4
0.8	692.5	647.2
0.9	703.7	663.8

Results and discussion

Based on the values of the thermodynamic parameters, the liquidus surface of the Ga–Sb–Zn ternary system is calculated and plotted in Fig. 2.

The invariant reactions in ternary Ga–Sb–Zn system are listed in Table 3, as well as the reaction temperatures and the types of those invariant reactions. It can be seen that in ternary Ga–Sb–Zn system there are eight invariant reactions: two eutectic (marked in Table 3 as type E) and six quasi-peritectic (marked as U), and eight regions of primary crystallization ((Sb), (Zn), GaSb, β , ε , δ , ζ , i , η).

Experimentally determined phase transition temperatures of the examined alloys, for all three characteristic

vertical sections of ternary Ga–Sb–Zn system, are presented in Table 4.

Three characteristic vertical sections of ternary Ga–Sb–Zn system were calculated, based on the literature data. The vertical sections were taken from all three corners, Ga, Sb, and Zn, with molar ratio equal to Sb:Zn = 1, Ga:Zn = 1, and Ga:Sb = 1, respectively.

Comparative review of the calculated phase diagrams for the three vertical sections together with experimentally determined phase transition temperatures by DTA and DSC methods, as a control of the quality of modeling, are presented in Fig. 3.

Two samples were investigated using SEM–EDS method and their compositions were presented in Table 5,

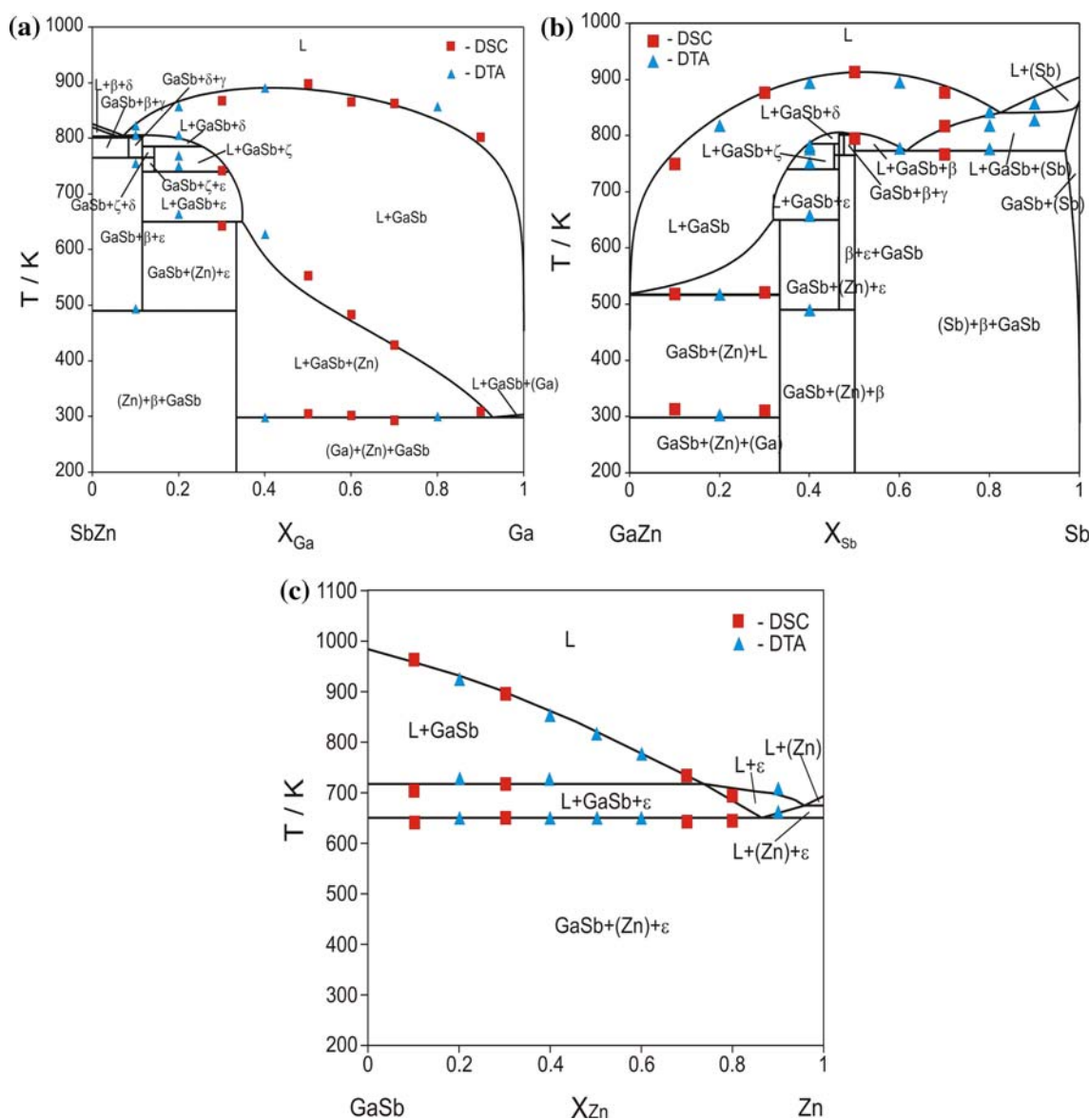


Fig. 3 Calculated phase diagrams for three vertical sections: **a** SbZn–Ga, **b** GaZn–Sb, and **c** GaSb–Zn

Table 5 Calculated and experimentally determined phase compositions in the ternary, Ga–Sb–Zn system at 673 K

Sample	Overall exp. composition (at.%)	Theoretic predicted phases	Experiment determined phases	Ga (at.%)		Sb (at.%)		Zn (at.%)	
				Exp.	Calc.	Exp.	Calc.	Exp.	Calc.
1.	18 Zn–61 Ga–21 Sb	GaSb	GaSb	50	50	50	50	0	0
		Liquid	Liquid	70	68	5	2	25	30
2.	40 Zn–28 Ga–32 Sb	Liquid	Liquid	7	10	3	4	90	86
		GaSb	GaSb	49	50	51	50	0	0
		ε	ε	2	0	41	42	57	58

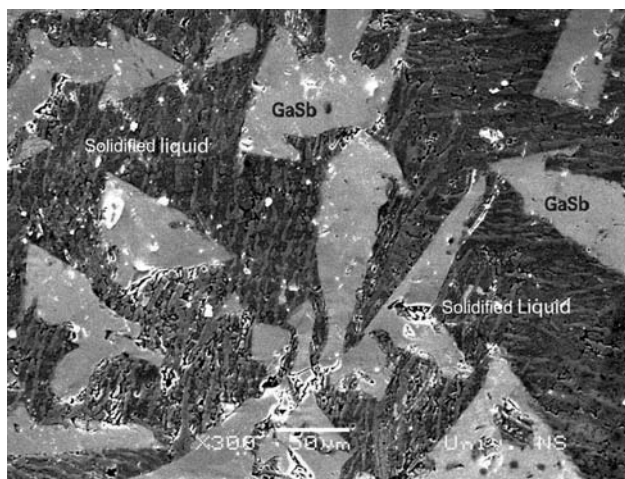
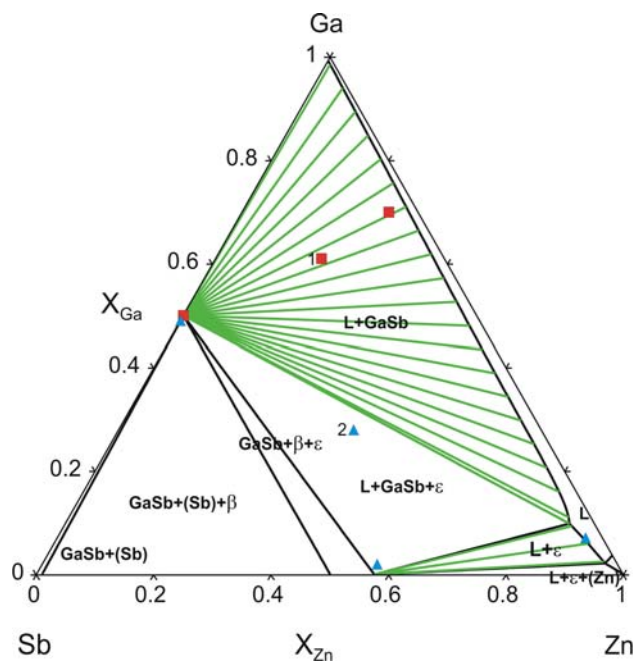
as well as calculated and experimentally determined (SEM–EDS) equilibrium compositions at 673 K.

On the temperature of 673 K, there is no diffusion of Zn observed in GaSb. Data for diffusion under isoconcentration conditions of Zn in GaSb were presented by da Cunha and Bougnot [21], in the temperature interval of 833–913 K, and maximum concentration $C_{Zn} = 1.1 \times 10^{21}$ atoms cm^{-3} is found for $T = 903$ K.

The microstructure of the sample 1 is shown in Fig. 4. The presence of two phases can be clearly seen on the microphotograph: GaSb and L.

The calculated isothermal section of the ternary Ga–Sb–Zn system at 673 K and experimentally determined phase compositions are presented in Fig. 5. The presence of the following crystallization fields: single phase field (L); three-two-phase fields ($L + \text{GaSb}$; $L + \varepsilon$; and $(\text{Sb}) + \text{GaSb}$) and four-three-phase fields ($\text{GaSb} + (\text{Sb}) + \beta$; $\text{GaSb} + \beta + \varepsilon$; $\text{GaSb} + L + \varepsilon$; and $L + \varepsilon + (\text{Zn})$) are observed.

It could be concluded that calculated and experimentally determined phase compositions are in relatively good agreement, as presented in Table 5 and Fig. 5.

**Fig. 4** SEM-micrograph of the sample 1**Fig. 5** Isothermal section of the ternary Ga–Sb–Zn system at 673 K and experimental values of the phase compositions for the samples 1 and 2 (full symbols are referred to the overall composition and empty on the compositions of single phase)

Conclusion

Phase diagram of the ternary Ga–Sb–Zn system was calculated using optimized literature data for thermodynamic parameters of the constitutive binary systems by CALPHAD method. It can be concluded that system has eight invariant reactions. By experimental verification by determined phase transformation temperatures, it can be concluded that the phase diagram is well calculated. There were also obtained good agreements of calculated and experimentally determined phase compositions on two investigated samples, whose compositions were in a region of vertical section at 673 K.

Acknowledgement This work was supported by Ministry of Science of the Republic of Serbia (Project No. 142043 and 142035B).

Calculations were performed by ThermoCalc and Pandat 8.1 softwares.

References

1. Bett AW, Keser S, Sulima OV (1997) *J Cryst Growth* 181:9
2. Bracht H, Nicols SP, Haller EE, Silveira JP, Briones F (2001) *J Appl Phys* 89(10):5393
3. Sundaram VS, Gruenbaum PE (1993) *J Appl Phys* 73(8):3787
4. Nicols SP, Bracht H, Benamara M, Liliental-Weber Z, Haller EE (2001) *Phys B Condens Matter* 308–310:854
5. Conibeer GJ, Willoughby AFW, Hardingham CM, Sharma VKM (1994) *Mater Sci Forum* 143–4(3):1427
6. Sulima OV, Bett AW (2001) *Sol Energy Mater Sol Cells* 66(1–4): 533
7. Luca S, Santailier JL, Rothman J, Belle JP, Calvat C, Basset G, Passero A, Khvostikov VP, Potapovich NS, Levin RV (2007) *J Sol Energy Eng, Trans ASME* 129(3):304
8. Adjadj F, Belbacha E, Bouharkat M, Kerboub A (2006) *J Alloys Compd* 419:267
9. Mirgalovskaya MS, Komova EM (1975) *Inorg Mater* 11:36
10. Lele S, Sarma BN (2009) *J Mater Sci* 44(9):2334. doi:[10.1007/s10853-008-3197-6](https://doi.org/10.1007/s10853-008-3197-6)
11. Tang JJ, Xue XA (2009) *J Mater Sci* 44(3):745. doi:[10.1007/s10853-008-3157-1](https://doi.org/10.1007/s10853-008-3157-1)
12. Munitz A, Bamberger M, Venkert A et al (2009) *J Mater Sci* 44(1):64. doi:[10.1007/s10853-008-3115-y](https://doi.org/10.1007/s10853-008-3115-y)
13. Avettand-Fenoel MN, Hadadi A, Reumont G et al (2008) *J Mater Sci* 43(5):1740. doi:[10.1007/s10853-007-2413-0](https://doi.org/10.1007/s10853-007-2413-0)
14. Ansara I, Chatillon C, Lukas HL, Nishizawa T, Ohtani H, Ishida K, Hillert M, Sundman B, Argent BB, Watson A, Chart TG, Anderson T (1994) *Calphad* 18:177
15. Dutkiewicz J, Moser Z, Zabdyr L, Gohil DD, Chart TG, Ansara I, Girard C (1990) *Bull Alloy Phase Diagr* 11(1):77
16. Liu XJ, Wang CP, Ohnuma I, Kainuma R, Ishida K (2000) *J Phase Equilib* 21(5):432
17. Dinsdale AT, Watson A, Kroupa A, Vrestal J, Zemanova A, Vizdal J (eds) (2008) *COST Action 531-Atlas of phase diagrams for lead-free solders, vol 1*. Brno, Czech Republic
18. Dinsdale AT (1991) *Calphad* 15(4):317
19. Hillert M, Staffansson LI (1970) *Acta Chem Scand* 24:3618
20. Sundman B, Agren J (1981) *J Phys Chem Solids* 42:297
21. da Counha SF, Bougnot J (2006) *Phys Status Solidi A* 22(1):205